

The surface tension of copper–nickel alloys

E. GORGES*, I. EGRY

Institute for Space Simulation, German Aerospace Research Establishment, DLR, 51147 Köln, Germany

The surface tension of copper–nickel alloys was measured, both as functions of concentration and temperature, using electromagnetic levitation and the oscillating drop technique. The measurements covered the entire concentration range from $c_{\text{Cu}} = 0$ to 100%, and a temperature range that included the molten as well as the undercooled regime. The results agree well with a model based on Butler's formula for the surface tension and chemical potentials measured in the bulk liquid phase. This allows one to calculate the surface segregation of this system.

1. Introduction

Copper and nickel are two metals with very similar properties. Fig. 1 gives a section of the phase diagram of copper–nickel alloys (after [1]). It shows that the system is perfectly miscible for all concentrations and at almost all temperatures.

Some properties of the components have almost the same value, at e.g. room temperature, the densities are

$$\rho_{\text{Cu}} = 8.96 \text{ g cm}^{-3} \quad (1)$$

$$\rho_{\text{Ni}} = 8.90 \text{ g cm}^{-3} \quad (2)$$

and molar volumes are

$$v_{\text{Cu}} = 7.09 \text{ mol cm}^{-3} \quad (3)$$

$$v_{\text{Ni}} = 6.60 \text{ mol cm}^{-3} \quad (4)$$

Despite of this similarity, the two materials have, in the liquid phase, different surface tensions, e.g. at 1400 °C, taken from [2] and [3]

$$\gamma_{\text{Cu}} = 1.240 \text{ N m}^{-1} \quad (5)$$

$$\gamma_{\text{Ni}} = 1.779 \text{ N m}^{-1} \quad (6)$$

Hence, one can hope to measure a strong concentration dependence of the surface tension of copper–nickel alloys, not being dominated by the bulk properties. For this reason, one may have a chance to find a simple model for the temperature and concentration dependence of the surface tension of this system.

2. Experimental procedure

The authors measured the surface tension by the levitated drop technique (see [4] and Fig. 2).

Two pieces of metal, one copper and the other nickel, are levitated by a strong magnetic field ($B \approx 10^{-2}$ T). Due to the resistivity of the materials, the samples heat up, melt and build one drop of

a copper–nickel alloy. The whole process takes place in a quartz–glass tube, which is filled with a mixture of helium and hydrogen. The temperature is measured by a pyrometer and controlled by the gas flow.

The oscillations of the levitated drop are filmed by a camera and recorded on a video tape. The time dependence of the cross-section, the radius in two directions at right angles and the movement of the centre of mass in two directions are evaluated by an image processing system. Fig. 3 shows a typical spectrum of a Cu (10 wt %) Ni alloy at $T = 1167$ °C.

Theory predicts that there are five peaks due to surface oscillations. Investigation of the sum and difference signal of the two radii allows the identification of the different modes [4]. After this procedure, one is able to calculate the surface tension, γ , according to

$$\gamma = M \frac{3}{32\pi} \left[\sum_{m=-2}^{m=2} \omega_m^2 - \omega_\tau \left(1.9 + 1.2 \frac{z_0^2}{R^2} \right) \right] \quad (7)$$

with

$$z_0 = \frac{g}{2\omega_\tau^2} \quad (8)$$

Here, ω_τ is the translation frequency, R the radius of the sample, M its mass and g the gravitational acceleration.

The first part of Equation 7 contains the frequencies ω_m of the different modes. It was derived by Lord Rayleigh [5] at the end of the last century under the assumption of no external forces acting on the sample. Cummings and Blackburn [6] gave a correction of this formula by taking the strong magnetic fields into account. The validity of this formula has been tested and confirmed by Sauerland *et al.* [3].

2.1. Measurements and model

A typical measurement for Cu (40 wt %) Ni is given in Fig. 4 by the dots. It shows that for this concentration

* Member of the "Graduiertenkolleg: Schmelzen, Erstarren und Grenzflächen". This work is supported by the "Deutsche Forschungsgemeinschaft DFG".

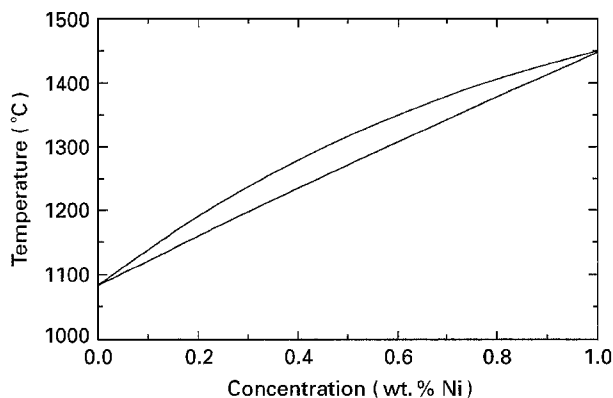


Figure 1 The phase diagram of copper–nickel, after [1].

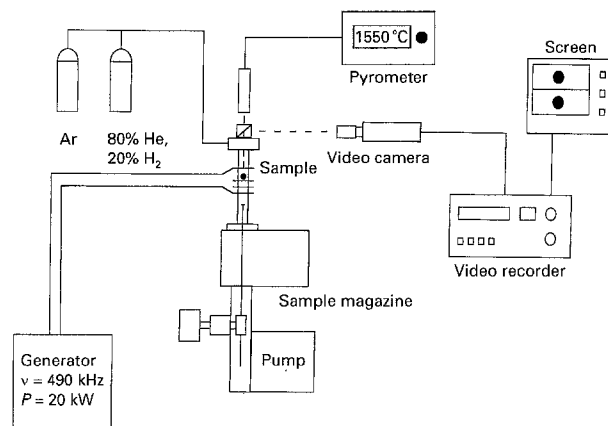


Figure 2 A sketch of the apparatus for levitation and the oscillating drop technique.

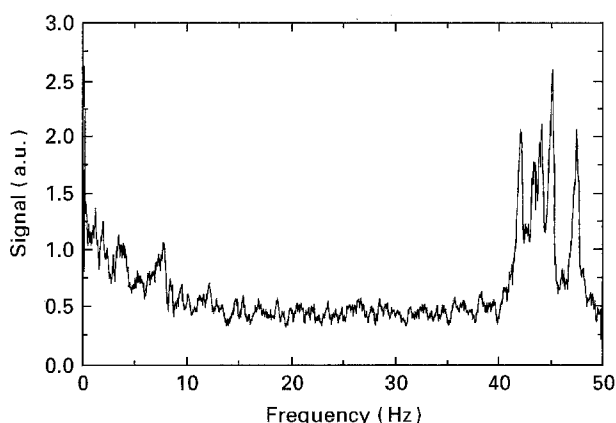


Figure 3 A typical spectrum of the surface oscillations of Cu(10 wt.% Ni) at $T = 1167^\circ\text{C}$. Here, five peaks are clearly visible between 40 and 50 Hz.

the temperature dependence of the surface tension in this range is almost linear. There is no different behaviour in the normal and supercooled state.

Starting from Butler's [7] equation for surface tension

$$\gamma = \frac{\mu_i^S - \mu_i^B}{a_i} \quad (9)$$

a model is developed. Equation 9 gives the surface tension as the difference of the chemical potentials of

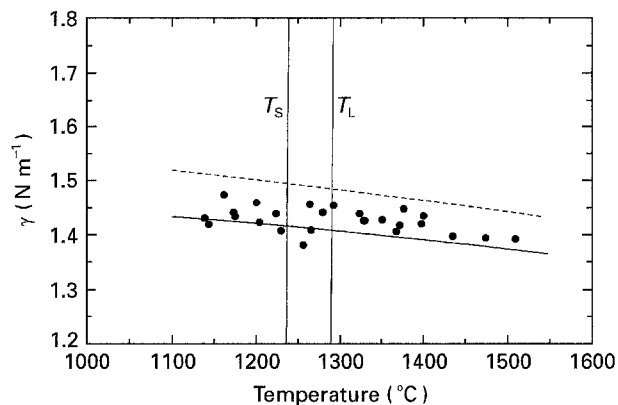


Figure 4 Temperature dependence of Cu (40 wt %) Ni compared with the ideal solution (dashed line) and subregular solution (solid line) model. This measurement contains surface tension values in the normal and supercooled state.

TABLE I Parametrization of the molar volumes of copper and nickel as used in the model (from [8])

Element	$v_{i,m}$ ($10^{-6} \text{ m}^3 \text{ mol}^{-1}$)	α_i (10^{-4} K^{-1})	$T_{i,m}$ (K)
Cu	7.94	1.00	1356
Ni	7.43	1.15	1728

the surface, S, and the bulk, B, divided by a factor, giving the number of atoms per surface area. The factor a_i can be calculated from [8]

$$a_i = 1.09 v_i^{2/3} N_A^{1/3} \quad (10)$$

with v_i being the molar volume and N_A the Avogadro constant. The procedure is now reduced to the problem of finding a model for the chemical potentials. For a mixture, they can be split into two parts

$$\mu_i^{S,B} = \mu_{i,\text{pure}}^{S,B} + \mu_{i,\text{mix}}^{S,B} \quad (11)$$

one being responsible for the pure component, the other for all mixing effects. This gives

$$\gamma = \frac{\mu_{i,\text{pure}}^S - \mu_{i,\text{pure}}^B}{a_i} + \frac{\mu_{i,\text{mix}}^S - \mu_{i,\text{mix}}^B}{a_i} \quad (12)$$

$$= \gamma_i + \frac{\mu_{i,\text{mix}}^S - \mu_{i,\text{mix}}^B}{a_i} \quad (13)$$

where the definition of the surface tension of a pure element is used. A first and very simple model can be made by taking the ideal solution model. This gives

$$\mu_{i,\text{mix}}^{S,B} = RT \log(c_i^{S,B}) \quad (14)$$

Here, the $c_i^{S,B}$ are the concentrations of the different materials. One obtains for the surface tension

$$\gamma = \gamma_1 + \frac{RT}{a_1} \log \frac{c_1^S}{c_1^B} = \gamma_2 + \frac{RT}{a_2} \log \frac{c_2^S}{c_2^B} \quad (15)$$

For the calculation of a_i , use Equation 10 and a parametrization of the molar volumes, given by Iida and Toshihiro (see Table I and [8])

$$v_i = v_{i,m} [1 + \alpha_i (T - T_{i,m})] \quad (16)$$

with $v_{i,m}$ being the molar volume at the melting temperature, $T_{i,m}$. The parameter α_i is the temperature

TABLE II The parametrization of the surface tension for the pure elements. For the element copper taken from [2], for nickel taken from [4].

Element	$\gamma_{i,0}$ (Nm ⁻¹)	β_i (10 ⁻⁴ Nm ⁻¹ K ⁻¹)	$T_{i,m}$ (K)
Cu	1.296	-2.34	1356
Ni	1.770	-3.30	1728

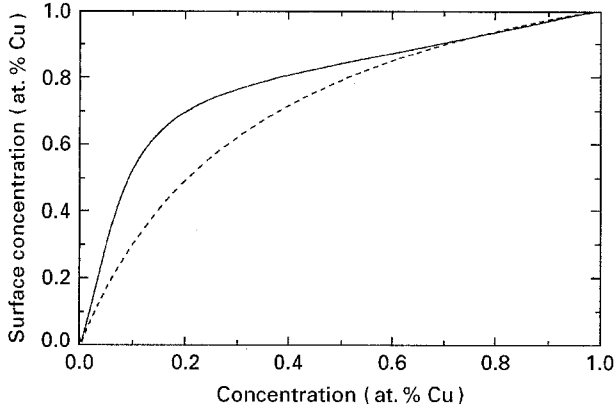


Figure 5 The surface segregation of copper, calculated for the ideal (dashed line) solution and subregular (solid line) solution model at 1550°C. The additional energies in the subregular solution model amplify the effect of surface segregation.

coefficient. The surface tension of pure copper and nickel are taken from [2] and [4]. They can be calculated by

$$\gamma_i = \gamma_{i,0} + \beta_i(T - T_{i,m}) \quad (17)$$

with $\gamma_{i,0}$ as the surface tension at the melting point, β_i as temperature coefficient and $T_{i,m}$ as melting temperature. The parameters are shown in Table II. Now everything is determined. From the second equality in Equation 15 one can calculate the surface concentrations for known γ_1, γ_2, a_1 and a_2 as a function of the bulk concentration and the temperature. Then, from the first equality, one can calculate the surface tension, γ .

This yields for the system Cu (40 wt. %) Ni the broken line in Fig. 4. It shows, that the agreement between measurement and this theory is very poor. The reason for this is that changes in the energy of the system (heat of mixing) were not taken into account.

The broken line in Fig. 5 shows the concentration dependent surface segregation of copper for a temperature of $T = 1550^\circ\text{C}$. As expected, the material with the lower surface tension segregates on the surface, minimizing its total energy. Brongersma *et al.* [9] have already studied and confirmed the surface segregation of copper by secondary ion mass spectroscopy (SIMS) for the solid state.

To get a better model and to compare the data with the parameters, measured for liquid bulk sample, one can go one step further and use the subregular solution model, developed by Hardy [10]

$$G_{\text{mix}} = Nc_1c_2[u_1 + (c_1 - c_2)u_2] + NkT(c_1\ln c_1 + c_2\ln c_2) \quad (18)$$

where G_{mix} is the Gibbs' free energy of mixing. The total Gibbs' free energy is given by

$$G_{\text{total}} = G_{\text{ideal}} + G_{\text{mix}} \quad (19)$$

No assumptions have to be made on G_1 and G_2 because these terms are responsible for the surface tension of the pure elements. They define the surface tensions, γ_1 and γ_2 . The u_i in Equation 18 are temperature dependent

$$u_i = u_{0,i} + Tu_{T,i} \quad (20)$$

The chemical potentials can be calculated by

$$\begin{aligned} \mu_1 &= \frac{\partial G_{\text{total}}}{\partial N_1} \\ &= \mu_{1,\text{pure}} + RT \log(c_1) \\ &\quad + c_2^2(u_0 + 3u_1) - c_2^3 4u_1 \\ \mu_2 &= \frac{\partial G_{\text{total}}}{\partial N_2} \\ &= \mu_{2,\text{pure}} + RT \log(c_2) \\ &\quad + c_1^2(u_0 + 3u_1) + c_1^3 4u_1 \end{aligned} \quad (21)$$

With Equation 13, one is able to calculate the surface tension (for further details see [8])

$$\begin{aligned} \gamma &= \gamma_1 + \frac{RT}{a_1} \log \frac{c_1^S}{c_1^B} + \frac{u_0 + 3u_1}{a_1} [\xi(c_2^S)^2 - (c_2^B)^2] \\ &\quad - \frac{4u_1}{a_1} [\xi(c_2^S)^3 - (c_2^B)^3] \end{aligned} \quad (23)$$

$$\begin{aligned} &= \gamma_2 + \frac{RT}{a_2} \log \frac{c_2^S}{c_2^B} + \frac{u_0 + 3u_1}{a_2} [\xi(c_1^S)^2 - (c_1^B)^2] \\ &\quad + \frac{4u_1}{a_2} [\xi(c_1^S)^3 - (c_1^B)^3] \end{aligned} \quad (24)$$

For the u_i , take the data given by Mey (see Table III and [11]). The number ξ gives the fraction of broken bonds in the surface. The best agreement between measurement and theory has been obtained for

$$\xi = \frac{3}{4} \quad (25)$$

Using this value, one can calculate, e.g. the temperature dependence of a Cu (40 wt %) Ni alloy, which is given in Fig. 4 as a full line. The agreement between theory and measurement is good.

The calculated surface segregation for a system at a temperature of 1550°C is plotted in Fig. 5 as a full line. One can see, that taking the subregular solution model, the effect of surface segregation is amplified.

Fig. 6 gives the concentration dependence of the surface tension at a constant temperature ($T = 1550^\circ\text{C}$).

TABLE III The parameters for the enthalpy of mixing for the copper-nickel system as used in the model (from [11])

i	$u_{0,i}$ (J mol ⁻¹)	$u_{T,i}$ (J mol ⁻¹ K ⁻¹)
1	12048.61	1.29093
2	-1861.61	0.94201

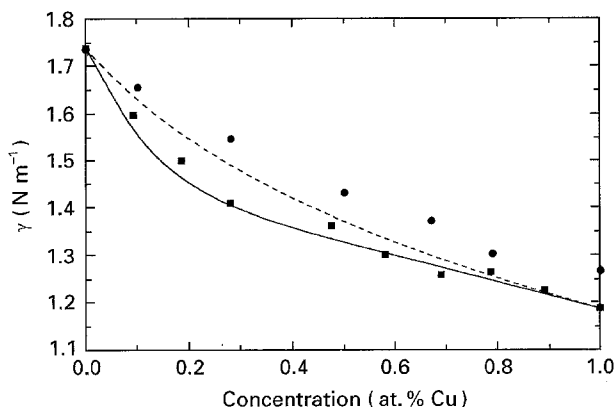


Figure 6 Concentration dependence of surface tension of Cu-Ni at 1550°C taking the ideal (dashed line) and subregular solution (solid line) model, compared with the authors' measurements (square symbols) and data taken from [12] (circular symbols).

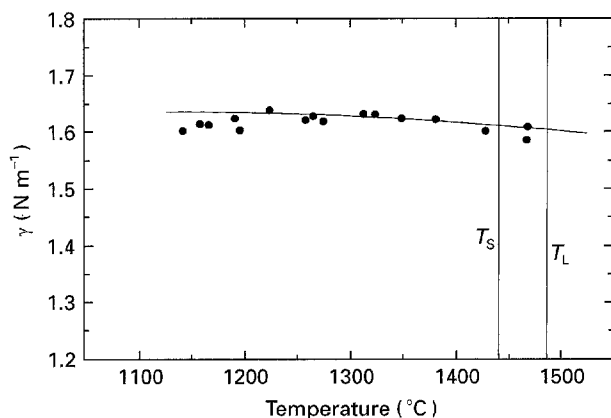


Figure 7 An effect of surface segregation. Despite the linearity of the energies in temperature, the temperature dependence of the surface tension of Cu (10 wt % Ni) is non-linear.

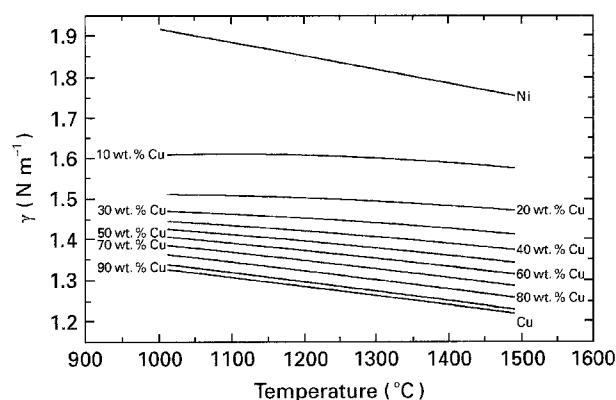


Figure 8 The temperature dependent surface tension for weight concentrations from 0 to 100% in 10% steps. One can see, that there is only a non-linearity in the temperature dependence for low copper concentrations.

The present measurements are shown as boxes and are compared to the two models ideal solution (broken line) and subregular solution (full line), as well as measurements of Fesenko and Eremenko [12] (dots).

It should be noted that the subregular model can lead to a non-linear temperature dependence of the surface tension of alloys, even with a linear temperature dependence of its pure constituents and the energies of mixing. This is confirmed by the authors' data, as shown in Fig. 7.

In Fig. 8, the temperature dependence of copper-nickel alloys is shown. This is plotted for weight concentrations from 0 to 100% in 10% steps. Only for low copper concentrations is a non-linear behaviour observed. The data is in full agreement with the authors' measurement.

3. Conclusions

The surface tension of copper-nickel alloys was measured. Then the authors showed, that a model, made of Bulter's equation for surface tension, Hardy's subregular solution model for chemical potentials and thermo-physical data for the bulk liquid is in good accordance with measured data, for the whole concentration and temperature range. Equations 23 and 24 can be taken to calculate the surface tension for a given temperature and concentration.

It should be mentioned, that there is no fitted parameter needed for this model. All the data is taken from literature in accordance with the phase diagram.

Out of this model, one is able to calculate the surface segregation. The differences between measurement and model, especially in Fig. 7, may be caused by the implicit assumption of a surface monolayer and differences in the energy parts of the Gibbs' free energy of the surface.

References

1. T. B. MASSALSKI, "Binary Alloy Phase Diagrams" (American Society for Metals, Metals Park, OH, 1986) p. 942.
2. I. EGRY, S. SAUERLAND and G. JACOBS, in "Proceedings of the 13th European Conference on Thermophysical Properties", Lisbon (1993) (to be published in *High Temp. High Pressure*).
3. S. SAUERLAND, R. F. BROOKS, I. EGRY and K. C. MILLS, in "Proceedings of the Fifth International Symposium on Experimental Methods for Material Science Research, Denver," edited by W. Hofmeister (The Minerals, Metals and Materials Soc., Warrendale, PA, 1993) p. 65.
4. S. SAUERLAND, K. ECKLER and I. EGRY, *J. Mater. Sci. Lett.* **11** (1992) 330.
5. LORD RAYLEIGH, *Proc. Roy. Soc.* **29** (1879) 71.
6. D. L. CUMMINGS and D. A. BLACKBURN, *J. Fluid Mech.* **224** (1991) 395.
7. J. A. V. BUTLER, *Proc. Roy. Soc.* **A132** (1932) 348.
8. T. IIDA and T. TOSHIRO, *Steel Res.* **1** (1994) 21.
9. H. H. BRONGERSMA, P. A. J. ACKERMANS and A. D. VAN LANGEVELD, *Phys. Rev.* **B34** (1986) 5974.
10. H. K. HARDY, *Acta Metall.* **1** (1953) 202.
11. S. AN MEY, *Calphad* **16** (1992) 255.
12. V. N. FESENKO and V. N. EREMENKO, *Zh. Fis. Khim.* **35** (1961) 860.

Received 19 July
and accepted 25 November 1994